Nano Science and Nano Technology
An Indian Journal

Trade Science Inc.

Electrical evaluation of scaled organic thin-film transistors with submicron-gap electrodes fabricated by focused ion beam sputtering

Yoshihiro Tada, Katsuhiro Uesugi, Hisashi Fukuda*
Division of Engineering for Composite Functions, Muroran Institute of Technology,
27-1 Mizumoto, Muroran, Hokkaido 050-8585, (JAPAN)
E-mail : fukuda@mmm.muroran-it.ac.jp

ABSTRACT

Submicron-gap electrodes were fabricated using focused ion beam (FIB) sputtering and applied as source/drain to scaled organic thin-film transistors (OTFTs). Fully focused Ga ions emitted from liquid ion source in a FIB system were irradiated onto a target metal surface for the etching of a defined area. A comparison of long-channel OTFTs indicates that with decreasing channel length toward submicron region, marked reduction of mobility and a threshold voltage shift were observed in submicron-channel OTFTs. A 0.25 µm-channel OTFTs fabricated by the FIB process showed a threshold voltage of -0.5 V and a carrier mobility three orders of magnitude smaller than that of the 5-µm-channel conventional OTFT. The 0.25 µm-channel OTFTs exhibit also a nonsaturating drain current in the output characteristics owing to short-channel effect. It was concluded that large contact resistance at the metal/organic interface provides the degradation of mobility of scaled OTFTs.　　　© 2012 Trade Science Inc. - INDIA

INTRODUCTION

The scaling down of metal-oxide-semiconductor field-effect transistors (MOSFETs) is of great importance in realizing next-generation ultralarge-scale integrated circuit (ULSI) systems. A goal of these devices are expected to realize a nano-dimensional quantum devices[1, 2]. Recently, various technologies for fabricating scaled-channel devices have been reported, with particular focus on the formation of nanogap electrodes. The electrodes will provide an application such as future molecular transistors and/or single dot nanomemories in the computer system. Several pro-cesses have been reported using mechanical break junctions[3], electromigration[4, 5], anisotropic chemical etching[6], and so forth. In addition, the analysis of carrier transport phenomena via nanosize quantum dots and/or molecular chains between nanogap electrodes is now in progress in the field of molecular electronics[7]. Another recently proposed application of small-gap electrodes is in next-generation display devices. Furthermore, the development of flexible flat-panel displays is expected to attempts to reduce the dimensions of organic thin-film transistors (OTFTs) to as small as possible[8, 9]. Although the behavior of scaled OTFTs is quite important to operate the large matrix display, system-

Full Paper

atical studies on the electrical properties of scaled OTFT have been reported quite few.

For the above purposes, a precise fabrication technology to obtain the three-dimensional fine structure is proposed in this study. Up to now, several important processes have been reported that use focused Ga ions emitted from ion source in a focused ion beam (FIB) system operating at a high voltage[10, 11]. In particular, material deposition and etching processes using an FIB may enable the precise fabrication of three-dimensional fine structures[12, 13]. In addition, it is a possible method of performing *in situ* observation through monitoring of secondary electrons, i.e., using scanning ion microscopy (SIM) system connected with an FIB apparatus. Of course, the patterning profile should be analyzed in nanometer order by methods based on scanning probe microscopy (SPM) including scanning tunneling microscopy (STM) and atomic force microscopy (AFM).

In this study, we will demonstrate the use of an FIB process for the fabrication of submicron-gap electrodes, which will be applied to fully scaled OTFTs with a submicron-length channel. We consider that the goal to use the FIB process is nanogap electrode fabrication for molecular devices and single dot nanomemories in future quantum computer system. In OTFTs, several organic materials have been investigated. In particular, pentacene thin film is the most promising organic material for scaled OTFTs, because of its high carrier mobility and long-term stability under atmospheric conditions, and its use is expected to make organic devices competitive with those based on standard amorphous silicon thin-film transistors. Therefore, we are focusing on the electrical properties of scaled OTFTs over wide range of channel lengths.

EXPERIMENTAL

The starting materials used in this study were Sb-doped, n^+-type (< 0.1 $\Omega \cdot$cm), Czochralski (CZ)-grown Si(100) wafers, which were cut into 1.5 cm $\times$ 1.5 cm chips as shown in Figure 1(a). These chips were rinsed in deionized water, ethyl alcohol, acetone, and then methyl alcohol, and were finally processed by a standard RCA method. After cleaning, the chips were treated in dry oxygen ambient at 1100 °C for 20 min to form a 200-nm-thick SiO_2 film (Figure 1(b)). Then,

triple-layered metal (Cr/Au/Cr) films were deposited on the SiO_2 film by vacuum deposition (Figure 1(c)). The thicknesses of the top Cr /Au/ bottom Cr layered film were 10, 40, and 5 nm, respectively. The middle Au film was used as an electrode. The bottom Cr film was necessary to maintain the adhesion of the metal film to the surface of the gate SiO_2 film. The top Cr film was prepared to prevent direct etching of the middle Au film by FIB tails in the following etching step. The films were then patterned to define 20-μm-wide strips
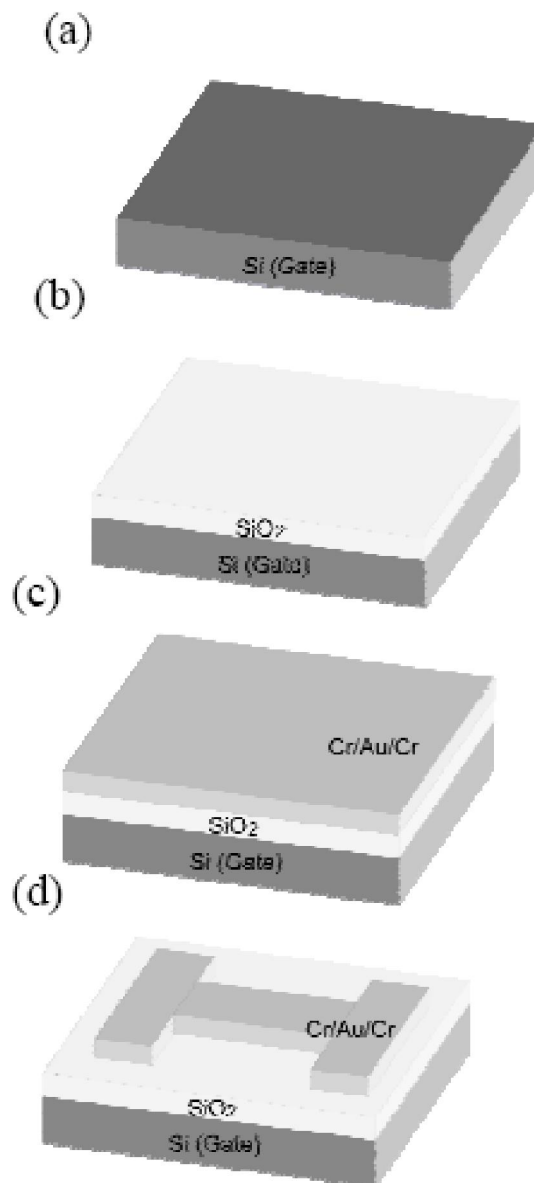

Figure 1 : Steps in the fabrication process of the electrode pattern. n^+-Si substrate (a), Formation of SiO_2 on the substrate (b), deposition of triple-layered metal (Cr/Au/Cr) films on the SiO_2 film (c), and patterning of films by photolithography (d).
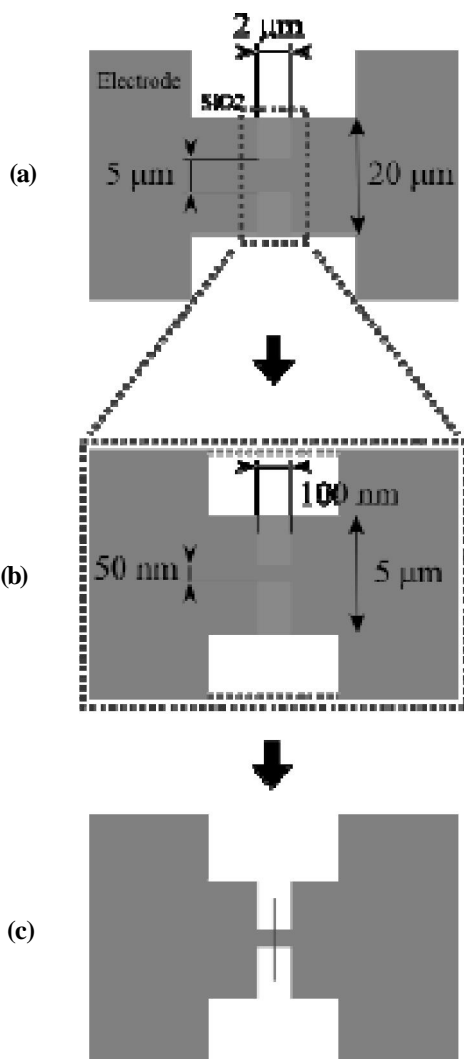
Hisashi Fukuda et al.

Figure 2 : An example for fine pattern fabrication of starting electrode pattern with width of 5 μm and length of 2 μm using FIB sputter etching. (a), patterning of metal film with width of 50 nm and length of 100 nm (b), and wire cutoff by single line scan (c).
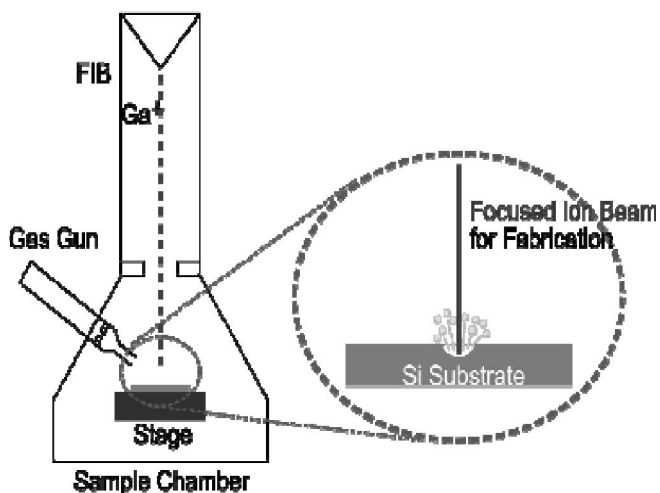

Figure 3 : Schematic drawing of FIB sputter etching.

by conventional photolithography (Figure 1(d)). An example of the submicron-gap electrode formation process, which involved three steps, is shown in Figure 2. In the first step, a starting electrode with a width of 5 μm and a length of 2 μm is prepared by photolithography (Figure 2(a)). In the second step, Ga^+ ions were irradiated to form fine pattern with a width of 50 nm and a length of 100 nm at the center of metal electrode (Figure 2(b)). In the final step, a small gap was formed in the patterned wire by a single line scan of focused Ga ions (Figure 2(c)).
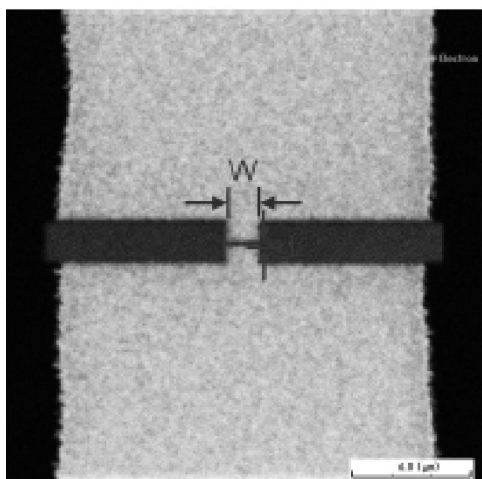
Figure 3 shows a schematic drawing of FIB sputter etching process, in which secondary electrons emitted from the material surface owing to Ga ion irradiation were detected by an SIM in a FIB system (SMI2050MU, SII Ltd). The surface morphology of the electrode after fabrication was imaged by AFM apparatus SPA300, SII Ltd., using a nonconductive tip in noncontact mode. X-ray diffraction (XRD) spectrometer (RIGAKU Ltd.) was used to analysis the molecular structure of the pentacene films. In this study, a 50-nm-thick pentacene layer was evaporated directly onto the top of the electrodes by vacuum evaporation at a condition of deposition rate of 4 Å/s under a pressure of 2.0×10^{-6} Torr at 300 K. The electrical characteristics of the OTFTs were measured using a computer-controlled automatic electrical analyzer system (Measure Jig Ltd, MI-494).
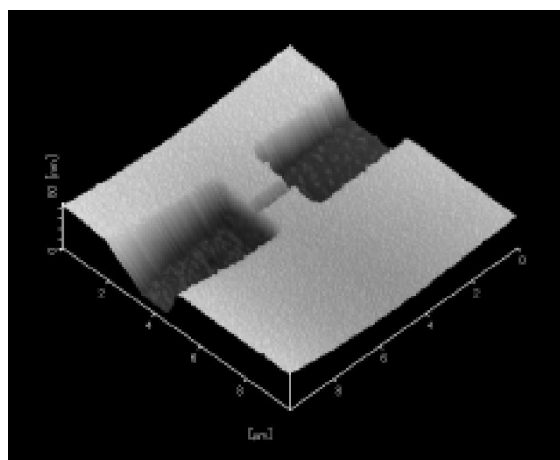
RESULTS AND DISCUSSION

Direct observation of the small-gap electrodes before the deposition of a pentacene film was performed by SIM method, where an obtained image is shown in Figure 4(a). The electrodes were successfully fabricated by a two-step process. First, a patterned bridge of width of 20 μm was fabricated by optical lithography, then the center of a wire was etched using the FIB to a width of 2 μm. Finally, the center of the electrode was cutoff to the desired length. Using the FIB process, a channel length of as low as 250 nm is fabricated.

Figure 4(b) shows a bird's-eye-view AFM image of the cutoff electrode pattern. The channel width and length were 2 μm and 0.25 μm, respectively. The depth around the center position was about 100 nm determined by a line profile obtained by AFM image scan-
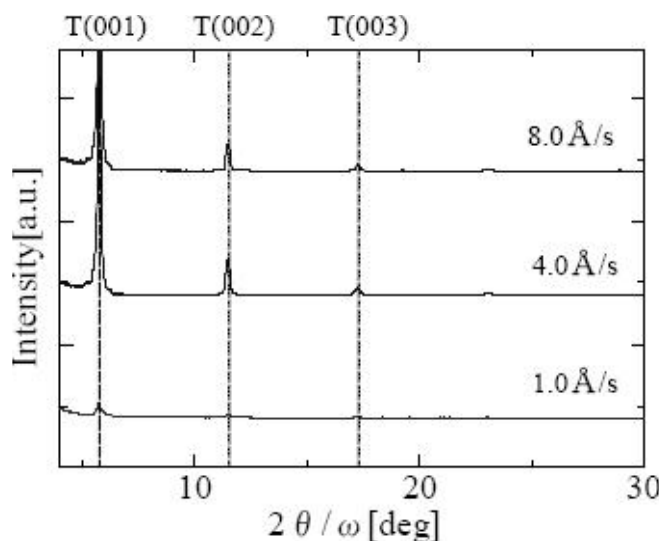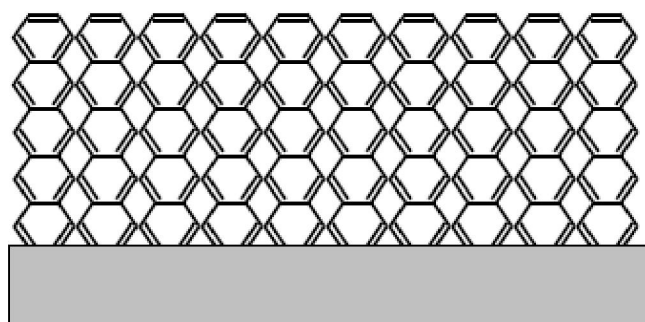
Figure 4 : SIM image of the electrode pattern after cutoff (a) and bird's-eye-view of the nanogap electrode obtained by AFM (b).

ning. After a pair of electrodes was fabricated, pentacene film was deposited in the active region to cover the surrounding area using a metal mask. XRD methods are extremely powerful in determining the degree of crystallinity, average domain size and film orientation. An in-plane X ray diffraction data of the pentacene films deposited on to the SiO_2 layer are shown in Figure 5 (a). The (001) diffraction peak located at $2\theta=5.7°$ corresponding to the interplanar pacing of 14.8 Å. The peaks of (002) and (003) are also found in the XRD spectra. Pentacene films have high crystalline ordering and crystal rods (c-axis) are well arranged almost normal to the surface. A schematic drawing is shown in Figure 5 (b), in which 50-nm-thick pentacene arranged in the "thin-film" phase. Then, the electrical properties of the OTFTs have been measured for the devices with various channel length.

Figure 5 : Dependence of the X-ray diffraction spectra on the growth rate for the pentacene thin films (a) and schematic drawing of the crystal arrangement of the pentacene thin films (b).

Figure 6 shows typical output and transconductance characteristics of an OTFT with a channel length L of 5 μm and channel width W of 20 μm. This device was fabricated by photolithography without FIB process. As can be seen in Figure 6(a), the output characteristics indicate long-channel-type operation in which the drain current and the hole injection occurs at a negative gate bias I_{ds} saturates at a high drain voltage V_{ds} operation. The carrier mobility μ$_{ext}$ in the saturation region is calculated using the equation[8].

$$I_{ds} = \frac{W}{2L} \mu_{ext} C_i \left(V_g - V_{th}\right)^2 \qquad (1)$$

Where V_g is the gate voltage and C_i is the capacitance per unit area of the gate insulator ($=3.4\times10^{-8}$ F/cm^2). V_{th} is the threshold voltage and is defined as the voltage at which the linear fit of $I_{ds}^{1/2}$-V_g intercepts the gate voltage axis. Using eq.(1), the calculated mobility
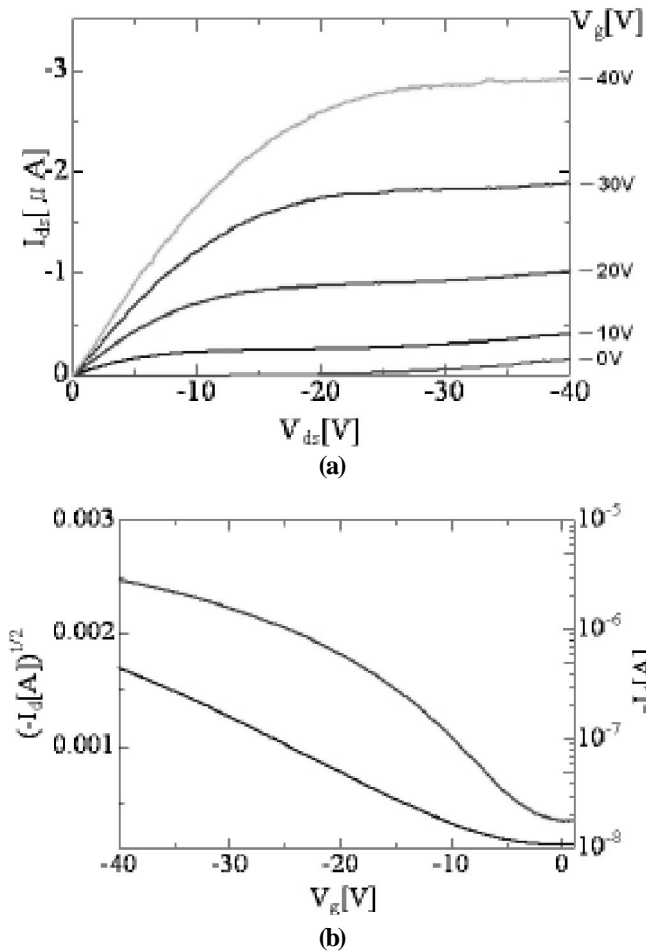
Full Paper

(a)

(b)

Figure 6 : I_{ds}-V_{ds} **characteristics (a) and transconductance characteristics (b) of a pentacene OTFT with** L=5 μm and W=20 μm.

Figure 7 : I_{ds}-V_{ds} **characteristics (a) and transconductance characteristics (b) of a pentacene OTFT with** L=0.75 μm and W=20 μm.

was 0.46 cm²/Vs. V_{th} is as -7.0 V for operation in an enhanced mode. The I_{on}/I_{off} ratio was obtained to be about 158 from the transconductance characteristics as shown in Figure 6(b).

Figure 7 shows the output and threshold voltage characteristics for an OTFT with channel length decreased to 0.75 μm. The carrier mobility and V_{th} were 1.16×10⁻³ cm²/Vs and -3.0 V, respectively. The I_{on}/I_{off} ratio increased to 1.8×10⁴ owing to the lower drain current around V_g =0. The result indicates the degradation of mobility and V_{th} at lower voltages with decreasing channel length.

Figure 8 shows the output and threshold voltage characteristics for a fully scaled OTFT decreasing a channel length to 0.25 μm. The results indicate that the carrier mobility and V_{th} were 2.48×10⁻⁴ cm²/Vs and -0.5 V, respectively. The I_{on}/I_{off} ratio was 1.0×10⁵. In the output characteristics, a gradual increase in drain

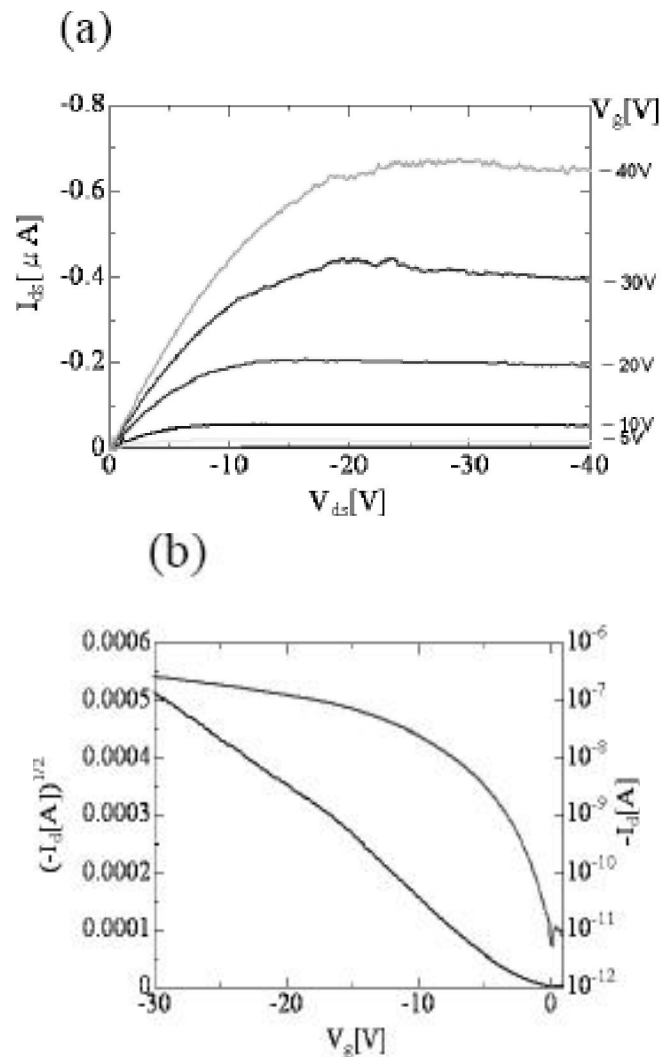current at a lower drain voltage and nonsaturation at a higher voltage were observed. For the MOSFETs, it is known that with decreasing channel length, the short-channel effect is enhanced[15]. As a result, the devices exhibit a degradation of mobility. However, a carrier mobility three orders of magnitude smaller than that of the 5-μm-channel OTFT could not be explained only by short-channel effect. In fact, submicron-channel MOSFETs indicated only one order of magnitude smaller mobility as compared to long-channel devices.

In an OTFT, the total device resistance R_{TOT} is given by[9].

$$R_{TOT} = R_{channel} + R_{contact}, \qquad (2)$$

Where $R_{channel}$ is the channel resistance and, $R_{contact}$ is the contact resistance at the organic/metal interface.
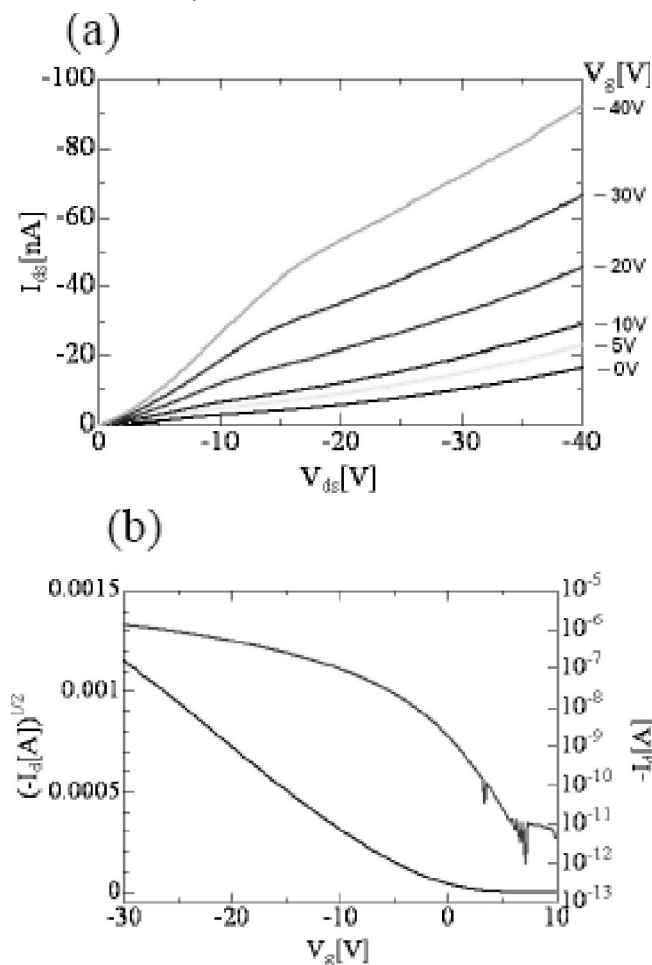
Full Paper

(a)

(b)

Figure 8 : I_{ds}-V_{ds} **characteristics (a) and transconductance characteristics (b) of a pentacene OTFT with** L**=0.25** μm **and** W**=2.0** μm**.**

With decreasing channel length, $R_{channel}$ is nearly to aero, thus, $R_{contact}$ becomes larger relative to $R_{channel}$. For example, the ratio of contact resistance to total resistance is about 50% in the micron-scale OTFTs. In contrast, when the channel length is reduced to 0.5 μm, the ratio of contact resistance to total resistance becomes nearly 100%. In eq.(2), putting R_{TOT} approximately equal to $R_{contact}$ for a 0.25 μm channel gives a contact resistance $R_c^{'}$ of about 6.6×10^5 Ωcm, where $R_c^{'}$ is defined as $R_{contact}$ (Ω)$\times W$ (cm). The total resistance R_{TOT} (=$R_{contact}$) is estimated from the linear region of the output characteristics of the OTFT at gate voltage V_g=0 V as shown in Figure 8(a). The value of $R_c^{'}$ is nearly the same as those of previously reported bottom-contact-type pentacene OTFTs[16]. It is concluded that high $R_c^{'}$ and then the degradation of mobility μ_{ext} are attributed to various scattering agents in the vicinity of the insulator interface, namely, charged centers, surface phonons, and surface roughness[17]. A conventional means of describing behavior is to introduce the mobility degradation factor θ, which in its simplest formulation leads to a mobility given by[17].

$$\mu_{ext} = \frac{\mu_{int}}{I + \theta(V_g - V_{th})} \qquad (3)$$

$$\theta = 2R_c^{'} \cdot \frac{W}{L} \mu_{int} C_i \qquad (4)$$

Assuming here that the intrinsic mobility μ_{int} of pentacene is about 0.1 cm²/Vs, then θ is calculated to be 180, and μ_{ext} is 2.8×10^{-4} cm²/Vs according to eq.(3), which is consistent with the experimentally obtained value. To maintain a mobility of 0.1 cm²/Vs even for the 0.25-μm-channel device, R_c must be suppressed to 10^3 Ωcm or below.

In Figure 8 (a), nonlinear build-up characteristics is observed. The conduction below V_{ds} =10 V is indeed not simple charge transport across a metal/organic interface, in which carriers must surmount the full potential barrier. Pentacene is a widely used *p*-channel organic semiconductor and Au is used to form an ohmic contact in pentacene OTFTs[9]. However, this is because the potential barrier at the pentacene/Au electrode interface modifies the carrier concentration, which is directly related to the value of R_c. Another possible injection mechanism involves defect-assisted transport, in which carriers bypass the barrier by hopping through midgap states between the LUMO (lowest unoccupied molecular orbital) and HOMO (highest occupied molecular orbital) levels. Details of the energy band scheme must be investigated to obtain scaled OTFTs with high performance.

In conclusion, a processing method for the fabrication of submicron-gate electrodes for application to scaled organic thin-film transistors (OTFTs) that involved focused ion beam (FIB) sputter etching was proposed. First, the electrical characteristics of OTFTs with channel length of 5 μm were examined, for which we obtained a carrier mobility of 0.46 cm²/Vs and a threshold voltage of -7.0 V. The values indicate that OTFTs with a micron-order channel exhibit normal long-channel behavior. In contrast, it was confirmed that submicron-channel OTFTs exhibited a non saturating drain current and a threshold voltage shift. In addition, the output characteristics indicated both anomalous cur-

Full Paper

rent build-up behavior not due to simple carrier transport in the drain current as well as the degradation of effective carrier mobility. In conclusion, by FIB processing, submicron-channel OTFTs were successfully fabricated, which revealed their unique characteristics of the mobility and threshold voltage being strongly affected by an increase in the channel electric field and enhanced contact resistance at the electrode/organic film interface.

REFERENCES

[1] G.Timp; Nanotechnology, Springer, New York, **(1998)**.

[2] D.A.Bernards, R.M.Owens, G.G.Malliaras; Organic Semiconductors in Sensor Applications, Springer, New York, **(2008)**.

[3] M.A.Read, C.Zhou, C.J.Muller, T.P.Burgin, J.M.Tour; Science, **278**, 252 **(1997)**.

[4] H.Park, A.K.L.Lim, A.P.Alivisatos, J.Park, P.L.McEuen; Appl.Phys.Lett., **75**, 301 **(1999)**.

[5] Z.M.Wu, M.Steinacher, R.Huber, M.Calame, S.J.Van Der Molen, C.Schonenberger; Appl.Phys.Lett., **91**, 053118 **(2007)**.

[6] K.Mimura, M.Ara, H.Tada; Mol.Cryst.Liq.Cryst., **472**, 63 **(2007)**.

[7] J.Park, A.N.Pasupathy, J.I.Goldsmith, C.Chang, Y.Yaish, J.R.Petta, M.Rinkoski, J.P.Sethna, H.D.Abruna, P.L.McEuen, D.C.Ralph; Nature, **417**, 722 **(2002)**.

[8] C.R.Kagan, P.And; Thin-Film Transistors, Marcel Dekker Inc., New York, **(2003)**.

[9] Z.Bao, J.Locklin; Organic Field-Effect Transistors, CRC Press, Boca Raton, **(2007)**.

[10] L.A.Giannuzzi, F.A.Stevie; Introduction to Focused Ion Beams: Instrumentation, Theory, Technique and Practice, Springer, New York, **(2005)**.

[11] J.Orloff, M.Utlaut, L.Swanson; High Resolution Focused Ion Beams: FIB and Its Applications, Kluwer Academic/Plenum Publishers, New York, **(2003)**.

[12] Y.Tada, K.A.Mohamad, K.Uesugi, H.Fukuda, E-Journal of Surf.Sci.and Nanotechnol., **8**, 250 **(2010)**.

[13] K.A.Mohamad, S.Yamada, K.Uesugi, H.Fukuda; E-Journal of Surf.Sci.and Nanotechnol., **7**, 808 **(2009)**.

[14] K.Kitagawa, T.Morita, S.Kimura; Thin Solid Films, **509**, 18 **(2006)**.

[15] T.Toyabe, K.Yamaguchi, A.Asai, M.S.Mock; IEEE Trans.Electron Devices, **ED-25**, 825 **(1978)**.

[16] K.P.Puntambekar, P.V.Pesavento, C.D.Frisbie; Appl.Phys.Lett., **83**, 5539 **(2003)**.

[17] K.Nomoto, N.Hirai, N.Yoneda, N.Kawashima, M.Noda, M.Wada, J.Kasahara; IEEE Trans.Electron Devices, **52**, 1519 **(2005)**.